ROYAL SOCIETY OF CHEMISTRY

PAPER

Check for updates

Nearly monodispersed, emission-tuneable conjugated polymer nanoparticles†

Struan Bourke,[a] Laura Urbano, [iD][b] Megan M. Midson, [iD][ac] Antoni Olona,[d] Basma Qazi-Choudhry,[a] Maryna Panamarova,[e] Ferran Valderrama,[d] Nicholas J. Long, [iD][c] Lea-Ann Dailey [iD][b] and Mark Green [iD]*[a]

Conjugated polymer nanoparticles have shown great promise in biological imaging due to their stable optical properties and inert composition but are usually polydispersed. By encapsulating conjugated polymer CN-PPV with a thin silica shell, it is possible to generate photo-stable, nearly monodispersed hollow nanoparticles with tuneable emission.

Conjugated polymer nanoparticles (CPNs) have emerged as a key imaging technology. Most optical imaging techniques employ organic fluorescent dyes as probes. Such dyes however, show limits such as unsatisfactory brightness, photobleaching and small Stokes shifts which result in a low limit of detection.[1] Consequently, materials that are bright whilst exhibiting improved photo-, bio-, and environmental-stability with a large Stokes shift are now under investigation for fluorescence microscopy and clinical imaging.[2] In recent years there has been a focus on the development of inorganic semiconductor quantum dots (QDs) which exhibit favourable optical properties.[3] However, as they are normally composed of heavy metals such as cadmium and selenium, there are concerns regarding toxicity and issues surrounding disposal.[4–6] Conjugated polymers are attracting attention due to their biocompatibility, superior optical properties and enhanced photostability.[7,8] Their wide range of biological applications include labelling,[9] imaging,[10] sensing,[11] and drug delivery.[12] A key drawback, however, is the lack of structural conformity in conjugated polymer nanoparticles when compared to quantum dots. In most cases, CPNs appear poly dispersed due to the lack of control over morphology during synthesis. Whilst the optical properties remain impressive, the varied particle sizes will ultimately present issues when the exact particle dimensions are required, for example, when the number of antibodies per particle are required, or when specific sizes are required for biological clearance. In an ideal scenario, it would be beneficial to have monodispersed particles composed of inert materials, that exhibited emission tunability like quantum dots.

Here, we describe a bioinspired silicification approach[13,14] (through nano-precipitation) to produce a set of silica-based monodispersed nanoparticles with a clear core/shell structure,[14–16] and we report the effect of different emissive polymer: capping agent ratios on the nanoparticle's optical characteristics. We obtained a variety of nearly monodispersed, colloidally stable hollow particles which exhibited high quantum yields and good photo-stability over time. Due to the preference for biological probes to emit towards the red end of the visible spectrum, we chose poly(2,5-di(hexyloxy)cyanoterephthalylidene) (CN-PPV). We further studied the ability of these nanoparticles as fluorescent probes by considering the uptake of the particles in HeLa cells. The ability to tune the wavelength without changing the chemical composition makes these organic nanomaterials particularly appealing for biomedical applications.

In brief, a typical preparation was carried out in a one-pot reaction as described in the supporting information. All reagents were dissolved in THF using differing ratios of the emissive conjugated polymer to Pluronic F127 capping agent (between 1:10 and 1:1000), and then injected into deionised water under sonication. The vial was left open to allow the THF to evaporate over four days.

Transmission electron microscopy (TEM) revealed core–shell structures, as shown in Fig. 1, with the silica shell appearing darker (due to higher electron density) compared to the PPO blocks of the Pluronic F127 and the conjugated

[a] *Department of Physics, King's College London, Strand, London, WC2R 2LS, UK. E-mail: mark.a.green@kcl.ac.uk*

[b] *Department of Pharmaceutical Sciences, University of Vienna, Althanstraße 14, 1090 Vienna, Austria*
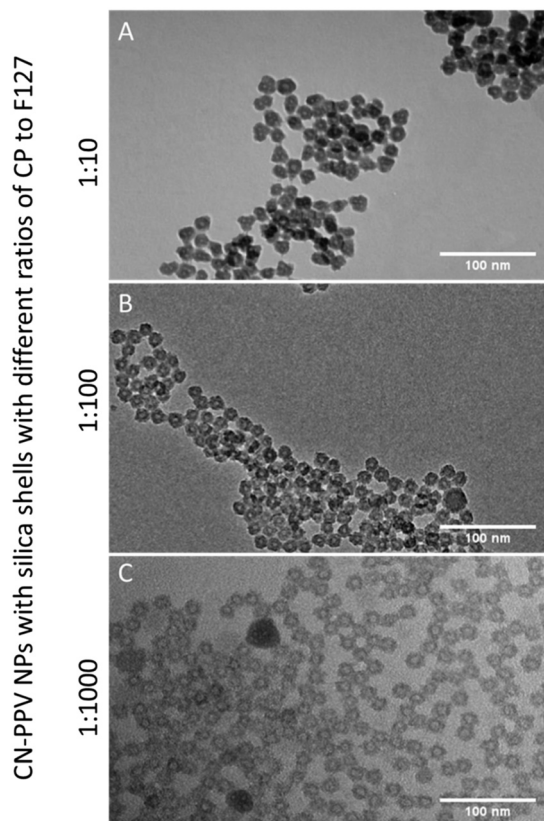
[c] *Department of Chemistry, Imperial College London, Molecular Sciences Research Hub, White City Campus, W12 0BZ, UK*

[d] *Cell Biology and Genetics Research Centre, St. George's University of London, London, SW17 0RE, UK*

[e] *Randall Division of Cell and Molecular Biophysics, Faculty of Life Sciences and Medicine, New Hunt's House, King's College London, Guy's Campus, London, SE1 1UL, UK*
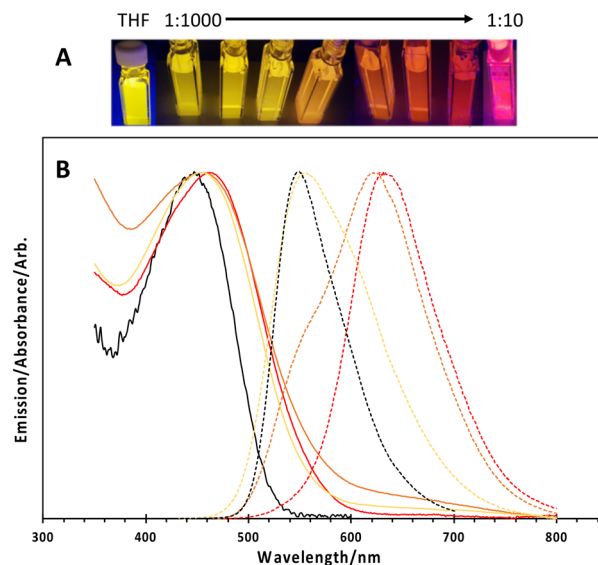
Fig. 1 Transmission electron microscopy images of CN-PPV nanoparticles with a silica shell, prepared with different ratios of conjugated polymer to Pluronic F127 capping agent. A) 1 : 10. B) 1 : 100. C) 1 : 1000. Scale bars = 100 nm.

Fig. 2 A) Image of conjugated polymer nanoparticles with differing polymer to Pluronic F127 ratios. B) Absorption (solid lines) and emission (dashed lines) of neat polymer in THF (black), and nanoparticles prepared with different conjugated polymer to Pluronic F127 ratios of 1 : 1000 (yellow), 1 : 100 (orange), 1 : 10 (red).

polymers. It is also noteworthy that there was no significant difference in the shape or size of the nanoparticles when comparing the different ratios of conjugated polymer to F127 used to manufacture the particles (Fig. 1 and S1†) and on average, the particles had a core diameter of 24 nm. We suggest the cores were comprised of the F127 and CN-PPV, whilst the shells were silica. The hydrodynamic diameters of the particles ranged between 30 and 80 nm with a PDI of *ca.* 0.16, depending on the reagent ratio (Fig. S2†). Lower conjugated polymer to F127 ratios resulted in an increase in hydrodynamic diameter, and a red shift in the fluorescence emission wavelength of CN-PPV as shown in Fig. 2. Such observations are consistent with a variation in the emitting polymer conjugation length, attributable to the tertiary structure of the polymer backbone, as previously noted on the behaviour of PPV derived polymers.[17,18] The particles were found to have a zeta potential value of *ca.* −10 kV.

How and why the nanoparticles formed a hollow relatively monodispersed morphology is currently unknown and will be explored The free polymer CN-PPV in THF has an absorption maximum at *ca.* 450 nm and an emission peak at *ca.* 550 nm. When prepared as nanoparticles described here, the emission could be tuned between *ca.* 550 nm (free polymer) and *ca.* 650 nm by tuning the ratio of conjugated polymer to Pluronic F127, as shown in Fig. 2. It is known that during

encapsulation, the conjugated polymer is forced to coil and twist, shortening its effective conjugation length and hence the observed shift in the emission wavelength. The associated absorption spectra exhibited a notable red shift and significant broadening, also shown in Fig. 2. This is again due to the increased inter-chateractions which allowed rapid energy transfer from high energy to lower energy segments due to the short-conjugated lengths and weakly emissive aggregates. Due to this forced coiling, the polymers interacted closely with each other causing delocalisation of the π-electrons, leading to an increased inter-chain aggregate state.[19] Numerous groups have reported similar observations based on the photo-physical behaviour of water-dispersed conjugated polymer nanoparticles.[3,16,20] These effects appeared to be independent of the silica shell, as nanoparticles prepared without the silica shell also displayed these optical shifts. The nanoparticle photo-stability over a period of 1 month was also explored. An aqueous suspension (3 mL) was stored in a quartz cuvette with a sealed lid, and the sample was excited at 450 nm periodically over a 35-day period, with 3 readings taken at each chosen day (Fig. S3†). It was shown that whilst there was a slight emission red shift, likely due to aggregation, the actual intensity of the sample did not vary significantly over the time period (dropping to 95% of the initial ($t = 0$) intensity). The quantum yield (QY) for CN-PPV in THF was calculated to be 59% as a dye comparison to rhodamine 6G.[21] The QY of the 1 : 10 CN-PPV NPs was 17% and the QY of the 1 : 1000 CN-PPV NPs was recorded as 51%. Particles without silica had QYs of 37%. The overall decreased quantum yield when compared to the free polymer was suggested to be attributed to defects in the polymers entrapped within the nanoparticles.
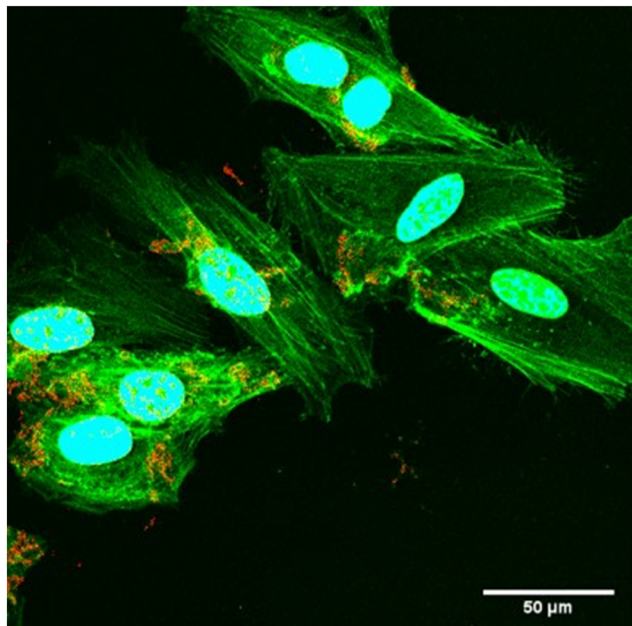
Fig. 3 Optical microscope image showing uptake of CN-PPV nanoparticles (CN-PPV : Pluronic F127 ratio of 1 : 10) in HeLa cells.

To investigate their potential use in biological imaging, the silica-shell passivated CN-PPV particles (1 : 10) were initially incubated with HeLa cells at a low concentration (1 μg ml^{-1} CN-PPV concentration) for 24 hours. After incubation, the cells were washed with PBS before being fixed in 10% formalin and the nucleus and actin were stained. Fig. 3 shows cellular uptake of the CN-PPV NPs at 60× resolution. The silica-shell cross-linked CN-PPV loaded particles (red) were either located on the surface of the HeLa cells or more likely were endocytosed by the cells although not taken into the nuclear area.

In conclusion, stable, brightly emissive, colour tuneable nanoparticles were successfully prepared by encapsulating CN-PPV in a silica-shell. By preparing these nearly monodispersed materials, a significant challenge in the preparation of biologically applicable nanoparticles has been addressed. Whilst conjugated polymer nanoparticles have excellent optical properties with almost unparalleled stability, the structural properties lag behind more established materials, such as quantum dots and gold nanoparticles. Whilst this might not immediately appear important in simple cellular imaging, to find true utility in routine advanced diagnostic applications, and ultimately in the clinic, materials must be prepared to a higher standard than is currently used. Anecdotal evidence has highlighted that numerous nanomaterials still struggle to find routine, reproducible use. Applications such as flow cytometry require a well-defined surface chemistry to avoid cross reactions and agglomeration, which is only possible with materials of a well-defined size. Likewise, if other more common tests (such as the now ubiquitous lateral flow assays) require quantitative or semi-quantitative outputs, a specific and constant particle morphology, and hence surface and targeting moieties will be essential. As we report here, entrapping the conjugated polymer within the silica shell, it was possible to provide small, relatively monodispersed, colloidally stable particles that had high quantum yields and good photo-stability over time. Upon incubation with HeLa cells, bright fluorescence was observed within the cells, particularly in the region surrounding the nuclei of the cells which suggests that uptake occurred. Further work will include adding a specific surface functionality that can allow monovalent interactions with required biological giving quantitative feedback on disease states.

Conflicts of interest

There are no conflicts to declare.

Acknowledgements

References

1 R. Reul, N. Tsapis, H. Hillaireau, L. Sancey, S. Mura, M. Recher, J. Nicolas, J. L. Coll and E. Fattal, Near Infrared Labeling of PLGA for in Vivo Imaging of Nanoparticles, *Polym. Chem.*, 2012, **3**(3), 694–702, DOI: **10.1039/c2py00520d**.

2 J. Yu, X. Zhang, X. Hao, X. Zhang, M. Zhou, C. S. Lee and X. Chen, Near-Infrared Fluorescence Imaging Using Organic Dye Nanoparticles, *Biomaterials*, 2014, **35**(10), 3356–3364, DOI: **10.1016/j.biomaterials.2014.01.004**.

3 P. Howes, M. Green, J. Levitt, K. Suhling and M. Hughes, Phospholipid Encapsulated Semiconducting Polymer Nanoparticles: Their Use in Cell Imaging and Protein Attachment, *J. Am. Chem. Soc.*, 2010, **132**(11), 3989–3996, DOI: **10.1021/ja1002179**.

4 L. Peng, M. He, B. Chen, Q. Wu, Z. Zhang, D. Pang, Y. Zhu and B. Hu, Cellular Uptake, Elimination and Toxicity of CdSe/ZnS Quantum Dots in HepG2 Cells, *Biomaterials*, 2013, **34**(37), 9545–9558, DOI: **10.1016/j.biomaterials.2013.08.038**.

5 R. Hardman, A Toxicologic Review of Quantum Dots: Toxicity Depends on Physicochemical and Environmental Factors, *Environ. Health Perspect.*, 2006, **114**(2), 165–172, DOI: **10.1289/ehp.8284**.

6 Y. Song, D. Feng, W. Shi, X. Li and H. Ma, Parallel Comparative Studies on the Toxic Effects of Unmodified CdTe Quantum Dots, Gold Nanoparticles, and Carbon Nanodots on Live Cells as Well as Green Gram Sprouts, *Talanta*, 2013, **116**, 237–244, DOI: **10.1016/j.talanta.2013.05.022**.

7 K. Pu, N. Chattopadhyay and J. Rao, Recent Advances of Semiconducting Polymer Nanoparticles in in Vivo Molecular Imaging, *J. Controlled Release*, 2016, **240**, 312–322, DOI: **10.1016/j.jconrel.2016.01.004**.

8 D. Tuncel and H. V. Demir, Conjugated Polymer Nanoparticles, *Nanoscale*, 2010, **2**(4), 484, DOI: **10.1039/ b9nr00374f**.

9 M. Green, P. Howes, C. C. Berry, O. Argyros and M. Thanou, Simple Conjugated Polymer Nanoparticles as Biological Labels, *Proc. R. Soc. A*, 2009, **465**(June), 2751–2759, DOI: **10.1098/rspa.2009.0181**.

10 X. Feng, Y. Tang, X. Duan, L. Liu and S. Wang, Lipid-Modified Conjugated Polymer Nanoparticles for Cell Imaging and Transfection, *J. Mater. Chem.*, 2010, **20**(7), 1312–1316, DOI: **10.1039/b915112e**.

11 Z. Tian, J. Yu, C. Wu, C. Szymanski and J. McNeill, Amplified Energy Transfer in Conjugated Polymer Nanoparticle Tags and Sensors, *Nanoscale*, 2010, **2**(10), 1999–2011, DOI: **10.1039/c0nr00322k**.

12 S. Saranya and K. V. Radha, Review of Nanobiopolymers for Controlled Drug Delivery, *Polym.-Plast. Technol. Eng.*, 2014, **53**(15), 1636–1646, DOI: **10.1080/ 03602559.2014.915035**.

13 H. Tan, J. M. Xue, B. Shuter, X. Li and J. Wang, Synthesis of PEOlated Fe3O4@SiO2 Nanoparticles via Bioinspired Silification for Magnetic Resonance Imaging, *Adv. Funct. Mater.*, 2010, **20**(5), 722–731, DOI: **10.1002/adfm.200901820**.

14 H. Tan, Y. Zhang, M. Wang, Z. Zhang, X. Zhang, A. M. Yong, S. Y. Wong, A. Y. Chang, Z.-K. Chen, X. Li, M. Choolani and J. Wang, Silica-Shell Cross-Linked Micelles Encapsulating Fluorescent Conjugated Polymers for Targeted Cellular Imaging, *Biomaterials*, 2012, **33**(1), 237–246, DOI: **10.1016/j. biomaterials.2011.09.037**.

15 C. Vauthier and K. Bouchemal, Methods for the Preparation and Manufacture of Polymeric Nanoparticles, *Pharm. Res.*, 2009, **26**(5), 1025–1058, DOI: **10.1007/s11095-008-9800-3**.

16 C. Wu, C. Szymanski and J. McNeill, Preparation and Encapsulation of Highly Fluorescent Conjugated Polymer Nanoparticles, *Langmuir*, 2006, **22**(7), 2956–2960, DOI: **10.1021/la060188l**.

17 S. V. Chasteen, S. A. Carter and G. Rumbles, The Effect of Broken Conjugation on the Excited State: Ether Linkage in the Cyano-Substituted Poly (p -Phenylene Vinylene) Conjugated Polymer Poly (2,5, 2′, 5′ -Tetrahexyloxy- 8, 7′ -Dicyano-Di- p -Phenylene Vinylene), *J. Chem. Phys.*, 2006, **124**(21), 214704, DOI: **10.1063/1.2196036**.

18 H. Chen, J. Zhang, K. Chang, X. Men, X. Fang, L. Zhou, D. Li, D. Gao, S. Yin, X. Zhang, Z. Yuan and C. Wu, Highly Absorbing Multispectral Near-Infrared Polymer Nanoparticles from One Conjugated Backbone for Photoacoustic Imaging and Photothermal Therapy, *Biomaterials*, 2017, **144**, 42–52, DOI: **10.1016/j. biomaterials.2017.08.007**.

19 K. Sun, H. Chen, L. Wang, S. Yin, H. Wang, G. Xu, D. Chen, X. Zhang, C. Wu and W. Qin, Size-Dependent Property and Cell Labeling of Semiconducting Polymer Dots, *ACS Appl. Mater. Interfaces*, 2014, **6**(13), 10802–10812, DOI: **10.1021/ am502733n**.

20 K. Li, J. Pan, S. S. Feng, A. W. Wu, K. Y. Pu, Y. Liu and B. Liu, Generic Strategy of Preparing Fluorescent Conjugated-Polymer-Loaded Poly(DL-Lactide-Co-Glycolide) Nanoparticles for Targeted Cell Imaging, *Adv. Funct. Mater.*, 2009, **19**(22), 3535–3542, DOI: **10.1002/adfm.200901098**.

21 I. D. W. Samuel, G. Rumbles and C. J. Collison, Efficient Interchain Photoluminescence in a High-Electron-Affinity Conjugated Polymer, *Phys. Rev. B: Condens. Matter Mater. Phys.*, 1995, **52**(16), R11573–R11576, DOI: **10.1103/ PhysRevB.52.R11573**.